ELSEVIER

Biochimica et Biophysica Acta 1384 (1998) 209–222

BIOCHIMICA ET BIOPHYSICA ACTA
BBA

E. coli HPII catalase interaction with high spin ligands: formate and fluoride as active site probes

M. Maj [a,1], P. Loewen [b], P. Nicholls [a,*]

[a] *Dept. Biol. Sciences, Brock University, St. Catharines, Ont., Canada L2S 3A1*
[b] *Dept. Microbiology, University of Manitoba, Winnipeg, Man., Canada*

Received 13 June 1997; accepted 26 August 1997

Abstract

E. coli catalase (HPII) wild type and mutant enzymes (heme d_{cis}-containing) were examined (i) to study the role of a distal haem cavity residue, asparagine-201, in high spin ligand binding and (ii) to compare the differences in this binding between heme d and protoheme enzymes such as that from beef liver (BLC). High spin fluoride complexes were formed by all three HPII catalases examined, wild type (201asn) and 201gln and 201asp mutants, but with a lower fluoride affinity than that of BLC. The binding of fluoride was pH-dependent, indicating that a proton is bound as well as a fluoride anion. HPII 201glu and 201asp mutants showed lower affinities for fluoride than did wild type, unlike their reactions with cyanide which are essentially independent of the nature of residue 201. The equilibria and rates of fluoride and formate binding to BLC were reexamined. The rates of reaction with formate were similar to those reported previously. Dissociation rates for fluoride-catalase are higher than for formate suggesting that the latter may be bound differently. High spin complexes between formate and all three HPII forms showed a substantially higher affinity than that of BLC for HPII wild type and progressively lower affinities for the two mutants. As with fluoride the reactions were pH-dependent, indicating that a proton is bound together with the formate anion (or that undissociated formic acid is the ligand). The known structures of the heme groups and heme pockets involved are discussed. Formate may be bound by secondary H-bonds within the heme pocket in both heme d_{cis} and protoheme enzymes. The nature of the heme pocket and the heme access channel may be more important than the chemical nature of the prosthetic group in controlling both high spin ligand interactions and reactions with the substrate hydrogen peroxide.

Keywords: Catalase; HPII; Peroxide; Catalatic reaction; Heme transformation; Protoheme; Heme d; Site directed mutagenesis; Reaction rate; Heme pocket; Formate; Fluoride; Distal residue; *(Escherichia coli)*

Abbreviations: BLC, beef liver catalase; HPII, hydroperoxidase II (catalase) of *E. coli*; WT, HPII wild type; N201Q, HPII mutant in which gln has replaced asn201; N201D, HPII mutant in which asp has replaced asn201; PVC, *Penicillium vitale* catalase; PMC, *Proteus mirabilis* catalase

* Corresponding author. Present address: Department of Biological Sciences, Central Campus, University of Essex, Wivenhoe Park, Colchester CO4 3SQ, Great Britain. Fax: +44-1206-872592; E-mail: pnicholl@essex.ac.uk

[1] Present address: Dept. Biochemistry, McMaster University, Hamilton, Ont, Canada L8N 3Z5.

0167-4838/98/$19.00
PII S0167-4838(97)00167-2

1. Introduction

Catalase, studied for over a century [1], was purified [2], crystallized [3] and analysed kinetically [4] at an early stage, but its mechanism of action remains problematic (cf. [5,6]). Primary sequences of over 100 heme-containing catalases from four kingdoms are known [7], and crystal structures have been determined for beef liver enzyme [8], *Escherichia coli* HPII [9], *Micrococcus lysodeikticus* catalase [10], *Penicillium vitale* catalase [11,12] and *Proteus mirabilis* catalase [13]. All contain four identical peptide subunits, each with a high spin heme prosthetic group. Beef liver [8] and *Micrococcus* [10] catalases contain protoheme whereas *Penicillium* and *E. coli* HPII [14] catalases contain heme d [15,16]. Amino acid sequences of these four enzymes show $\approx 70\%$ homology and their tertiary structures are similar. Tyrosyl always occupies the heme iron 5th coordination site [17] and the 6th site is vacant [18]. All catalases have an essential distal histidine and asparagine [16,17] but their activities, peroxide reactivities and ligand binding behaviours differ.

E. coli K12 HPII [19] is the best-characterized heme d_{cis} catalase [20]. Distal his128 is absolutely required and distal asn201 is partially needed for conversion of protoheme to heme d [16]. The N201A mutant contains mostly heme d and is partially active; N201H has protoheme and very limited activity. Conversion to a heme d like form occurs when N201H is treated with continuously generated peroxide [16,21].

All catalases dismute pairs of hydrogen peroxide molecules to oxygen and water – the catalatic process. The first H_2O_2 molecule oxidizes heme to compound I and the second reduces it back to the ferric state. One-electron reduction of compound I in protoheme enzymes yields inactive compound II. This process has not been identified in the heme d enzymes [21]. Hydrogen bonding of substrate to distal histidine and asparagine may occur during formation of compound I [17] as well as interactions with heme iron. A subsequent step gives a single iron-bound oxygen atom (Fe^{IV}) state and a π-cation porphyrin ring radical, releasing a water molecule.

The spontaneous transition of compound I to compound II and the decay of compound II are accelerated by high-spin ligands such as fluoride but not by cyanide [22]. As high-spin ligands apparently have similar affinities for free enzyme, compound I and compound II [22] the stabilities of the complexes may depend energetically on the heme pocket environment rather than upon the oxidation state of the iron. This possibility can be studied by comparing the ligand-binding behaviour of heme d and protoheme enzymes. A previous paper [23] examined binding of the low-spin ligand cyanide by HPII and its mutants. The present paper compares the binding of the high spin ligands fluoride and formate by this enzyme family with that of the classical beef liver enzyme. The results have been the subject of preliminary reports [24,25].

2. Materials and methods

2.1. Materials

Beef liver catalase (EC 1.11.16, $65\,000\,U\,mg^{-1}$) was from Boehringer Mannheim Biochemica, Montréal, Que., Canada. The crystalline suspension was diluted in sodium borate/HCl buffer (pH 8.25) and centrifuged at low speed for 3 min to remove insoluble material. Catalase (hematin) concentration was determined spectrophotometrically using an extinction coefficient of $120\,mM^{-1}\,cm^{-1}$ at 406 nm [26].

E. coli HPII catalases were obtained in the Department of Microbiology, University of Manitoba. Catalase (hydroperoxidase II or HPII) was isolated from *E. coli*, purified from strain UM255 and transformed with pAMkatE22 a plasmid containing the katE gene which encodes for the 753 amino acid protein [19]. Oligonucleotide-directed mutants of HPII were prepared in Manitoba as described by Loewen et al. [16]. The oligonucleotides were synthesized on a PCR-Mate synthesizer. The mutant sequences were confirmed by the Sanger method on single-stranded DNA from the same phagemids. The mutagenized fragments were reincorporated into pAMkatE72 and transformed into UM255 for expression. Concentrations of HPII (hematin) were estimated using the extinction coefficient reported in [27] of $118\,mM^{-1}\,cm^{-1}$ at 405 nm. The lyophilized protein was diluted in potassium phosphate buffer and centrifuged to remove insoluble material.

30% hydrogen peroxide was from Fisher Scientific. KH_2PO_4 was a product of J. T. Baker Chemical (Phillipsburg, NJ, USA) and K_2HPO_4 a product of Caledon Laboratories (Georgetown, Ont.). Sodium fluoride and sodium formate were AnalaR™ products from BDH (Poole, UK). All other chemicals were of analytical grade and purchased either from BDH or from Sigma (St. Louis, Mo, USA).

2.2. Spectroscopy

Spectra of beef liver catalase, HPII wild-type catalase and HPII mutants and their derivatives were obtained at Brock University either with a Beckman DU-7400 diode array spectrophotometer or with a Beckman DU-7HS spectrophotometer linked to Apple IIGS and Macintosh™ computers for data transfer into Deltagraph™ 2.0 spreadsheets. Concentrations of catalase employed varied from 4–10 μM (hematin). All experiments were carried out at 30°C in 100 mM potassium phosphate buffer at pH 5.0, 5.8 or 6.8 except where indicated otherwise. Kinetics of H_2O_2 decomposition [28] were monitored using an Olis™-Aminco™ double beam DW-2 spectrophotometer linked to a Compaq™ 286 computer employing Olis™ fitting routines for exponential decays.

Stopped flow kinetic measurements were performed using an Olis™ Durrum™ D-100 stopped flow spectrophotometer linked to a DOS-type 386 computer, analysing the data with the Olis™ fitting routines. Rates of catalase complex formation with fluoride and formate were determined at 23°C in 50 mM potassium phosphate buffer. Spectral and kinetic graphical analysis employed Deltagraph™ 2.0 or 4.0 Macintosh™ software.

2.3. Molecular modelling

Catalase structures were displayed and distances and configurations calculated using Quanta™ release

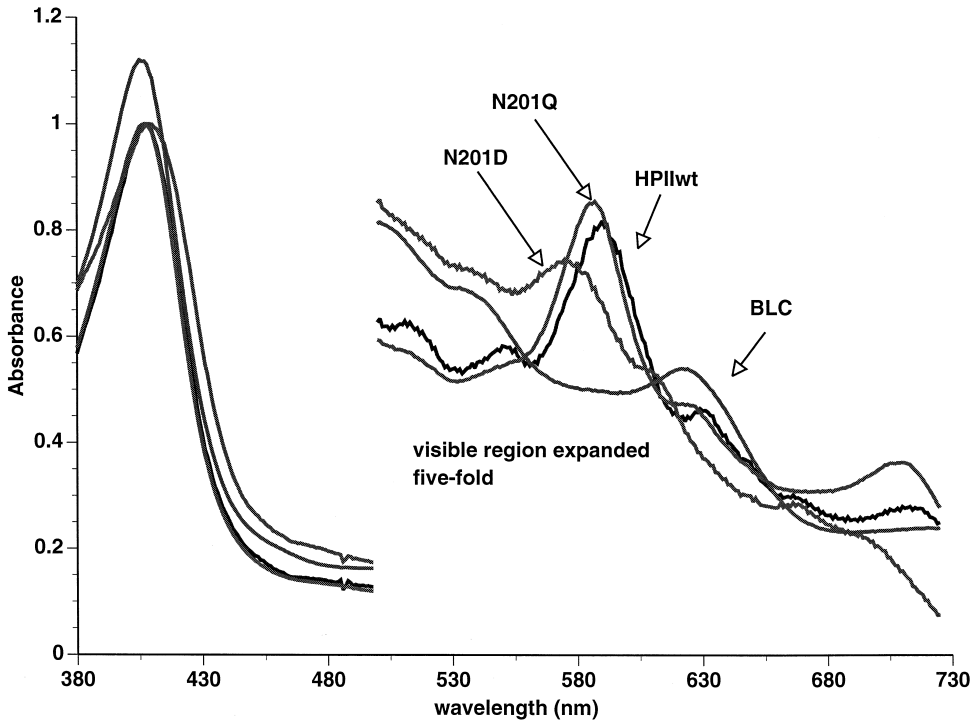

Fig. 1. Spectra of HPII wild-type, N201D and N201Q catalases. Absolute spectra of beef liver (dark gray), HPII wild-type (black), HPII N201D mutant (dark gray) and HPII N201Q mutant (light gray). The spectra were obtained with 4–10 μM (hematin) catalases in 100 mM potassium phosphate at pH 5.0, 23°C. The Soret maxima have been adjusted to equivalent molar optical densities (a common 10 μM hematin level).

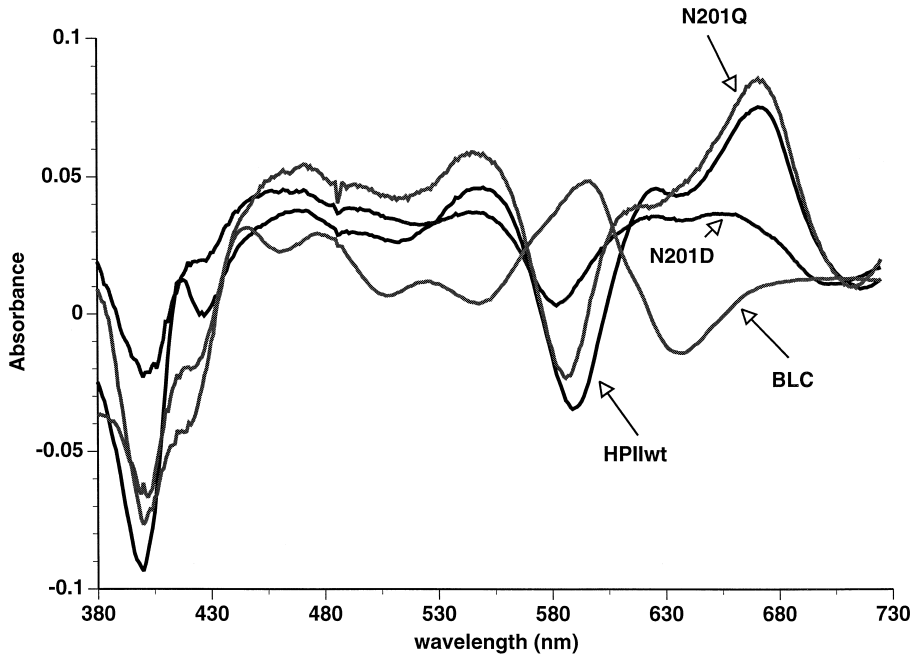

Fig. 2. Difference spectra of catalase-fluoride complexes. Difference spectra were obtained by sequential additions of aliquots of fluoride to each catalase sample. The medium contained 100 mM potassium phosphate pH 5.0 at 23°C. Other conditions are as in Fig. 1. BLC, beef liver catalase, sodium fluoride up to 19 mM. HPIIwt, HPII wild-type catalase, sodium fluoride up to 19 mM. N201D, HPII asn201asp mutant, sodium fluoride up to 4.3 mM. N201Q, HPII asn201gln mutant, sodium fluoride up to 24 mM. Difference spectra are calculated for the expected absorbance change at maximal complex formation.

4.1.1 version 95.0320 software (The University of York, York, England, Molecular Simulations Inc., 1984-1994) which functions on a UNIX operating system, Silicon Graphics Indigo2™ R4400 work station. Quanta™ allows for the manipulation of a molecule in 3-D space. It also allows for selective displaying, coloring and overlaying structures as well as creating graphical objects. Quanta release 4.1.1 includes CharmM™ dynamics calculations whose simulations permit energy minimization and hydrogen bond calculations.

3. Results

3.1. Spectra of catalase–fluoride complexes

The absorption spectra of the catalases used are shown in Fig. 1. Protoheme-containing beef liver

Table 1
Spectra and affinities of catalase-fluoride complexes

Catalase	Spectral maxima		Dissociation constants (mM)	
Type	Soret region (nm)	Visible region (nm)	pH 5.0	pH 5.8
BLC	407	596	3.5	23
HPII (WT)	410	551, 628, 671	0.16	ND
N201D	411	540, 612, 665	6.0	ND
N201Q	409	549, 625, 670	0.6	ND

Spectral analysis was performed in 100 mM potassium phosphate buffer at 23°C. Dissociation constants were obtained from fitted data collected from Fig. 3 and similar experiments at pH 5.0 and pH 5.8. BLC = beef liver catalase; HPII(WT) = *E. coli* HPII catalase with asn201; N201D = *E. coli* HPII catalase with asp201; N201Q = *E. coli* HPII catalase with gln201.

enzyme has a 405 nm Soret band and a 3-banded high spin ferriheme visible spectrum (500, 540 and 622 nm peaks). Heme d-containing HPII enzymes show an almost identical Soret band but a three-banded visible region spectrum shifted about 90 nm towards the red (590, 630 and 715 nm peaks). The relative intensities of the three visible region bands are also different, the highest energy transition at 590 nm being much more conspicuous than the presumed corresponding 500 nm transition in protoheme catalase.

Mutation of distal asparagine-201 to glutamine (N201Q) induces a slight blue shift of the visible region spectral bands without affecting the Soret peak position. The N201D (asn–asp) mutant had a broader

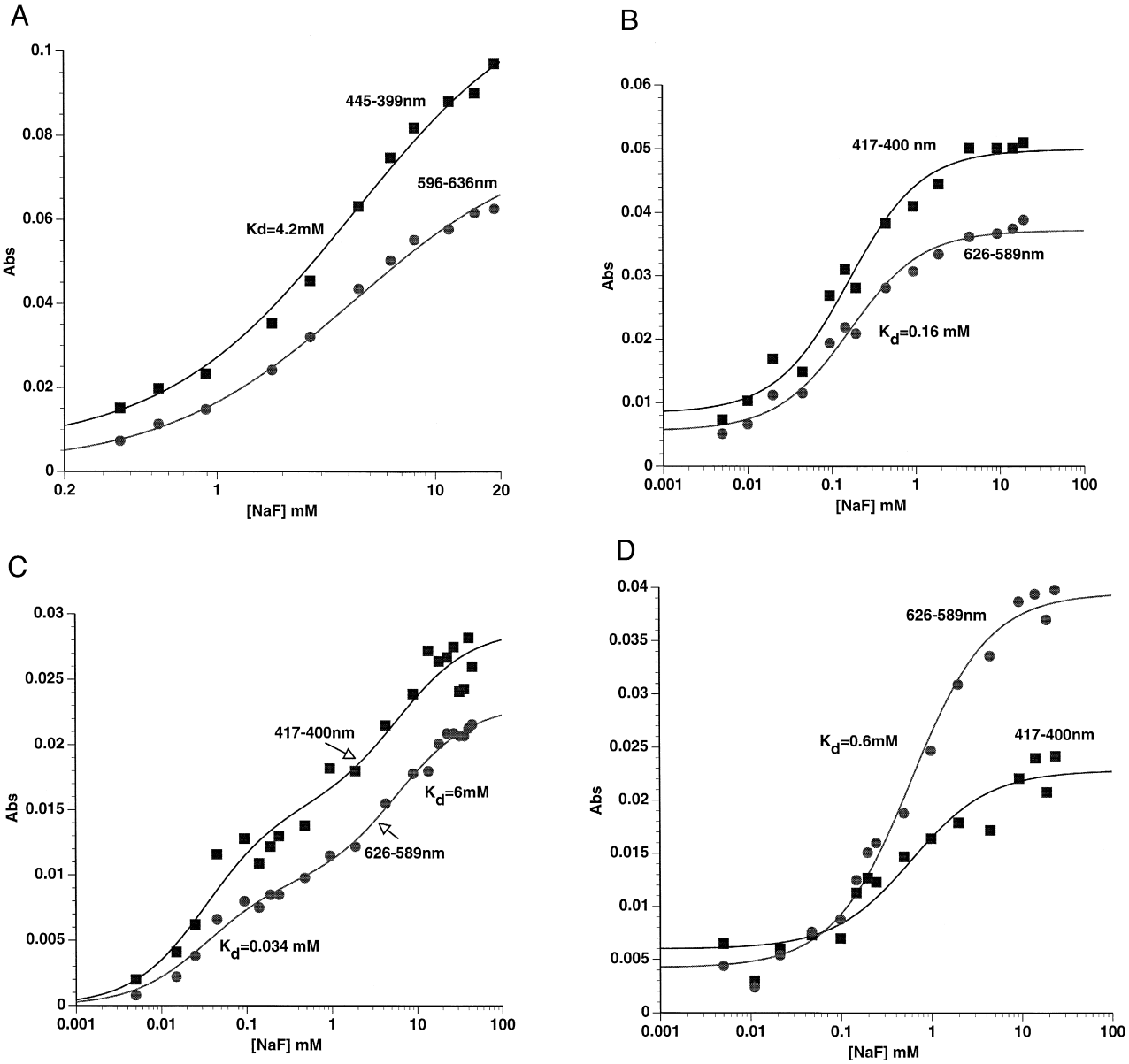

Fig. 3. Fluoride binding by catalases (A) beef liver catalase, wavelength pairs 445–399 nm (■) and 596–636 (●); (B) HPII wild-type, wavelength pairs 470–400 nm (■) and 670–710 nm (●); C. HPII N201D, wavelength pairs 450–400 (■) and 655–700 nm (●); D. HPII N201Q, wavelength pairs 470–400 nm (■) and 670–710 nm (●). Absorbance changes are plotted against log[fluoride] concentration. 100 mM potassium phosphate pH 5.0 at 23°C (assay conditions as in the legend of Fig. 2).

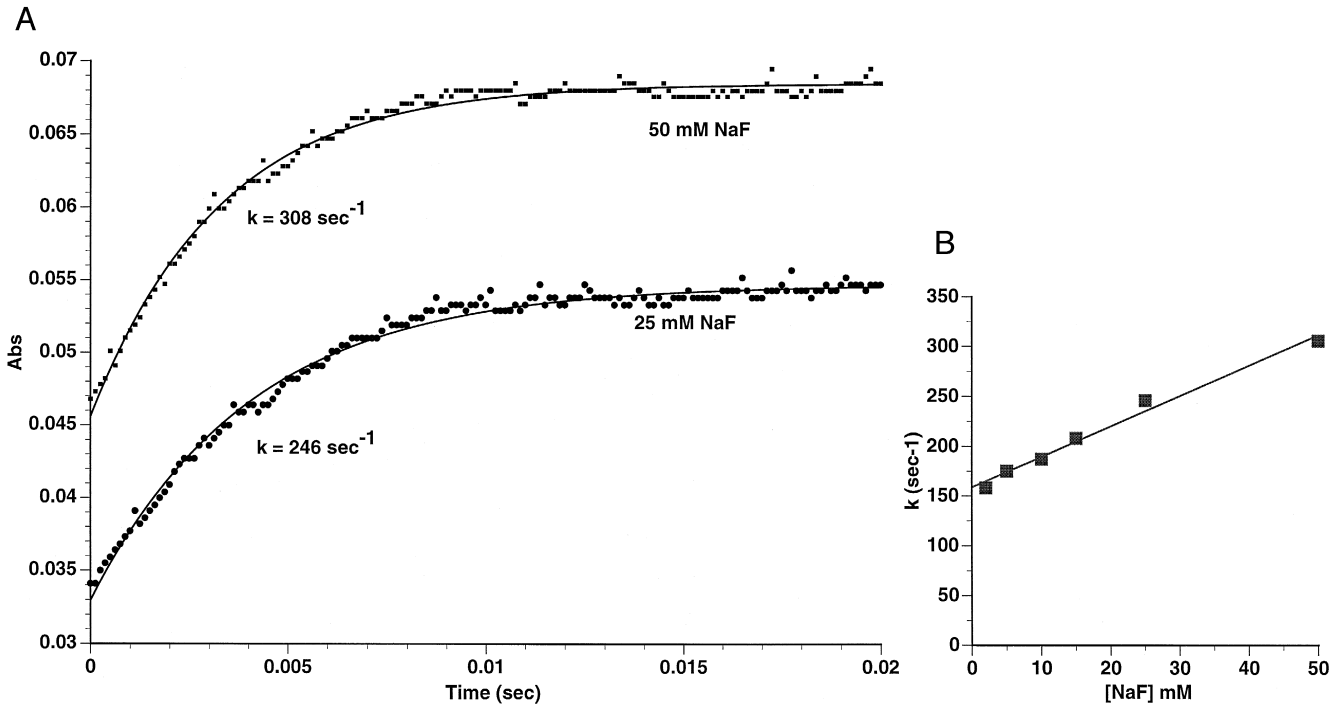

Fig. 4. Kinetics of fluoride binding: beef liver catalase. (A) Time courses of fluoride binding. Fluoride binding to 9 μM catalase was monitored with 50 mM (■, upper trace) and 25 mM NaF (J, lower trace) in the stop-flow spectrophotometer in 50 mM potassium phosphate buffer pH 5.8 at 23°C. The absorbance differences at 595–634 nm were fitted to single exponentials as shown. Reaction curves at 595 nm and 634 nm with sodium fluoride additions from 1–100 mM. (B) Rate constants for fluoride binding. First order rate constants plotted against the fluoride concentration. The rate constant at each [NaF] was obtained by a single exponential fit as in Fig. 4(A).

Soret band and a visible spectrum suggesting that full transformation to heme d may not have been achieved in this sample [16].

3.2. Equilibria of catalase-fluoride complexes

Difference spectra for the catalase-fluoride complexes are shown in Fig. 2. The 622 nm band of beef liver catalase is blue shifted and the Soret band slightly red shifted by fluoride, indicating high spin complex formation. The HPII catalase Soret band is red-shifted by 4 nm from its wild-type position and both wild-type and N201Q mutants show an α band blue shift from 710 to ≈670 nm. The N201D α-band shows a more modest blue shift. HPII catalases also exhibit subsidiary bands at 550 and 625 nm without counterparts in the protoheme catalase–HF complex (Table 1).

Absorbance changes at appropriate wavelength pairs were plotted against the logarithm of the fluo-

Table 2
Rates of fluoride and formate binding to beef liver catalase

Catalase species	pH 7.4			pH 5.8
	k ($M^{-1}s^{-1}$)	k_{min}(s^{-1})*	K_d (mM)	K_d (mM)
Ferric	160 $M^{-1}s^{-1}$	–	23	0.53
Comp. I (H_2O_2)	237 $M^{-1}s^{-1}$	0.1	–	–
Comp. I (PerA)	161 $M^{-1}s^{-1}$	0.007	–	–
Comp. II (PerA)	0.06 s^{-1} [c]	0.0005	>>50 [b]	6.0 [b]

[a] k_{min} = spontaneous peroxide compound reduction by endogenous donor.
[b] Affinity of compound II for formate is calculated from the catalysis of reduction by endogenous donor.
[c] Maximal endogenous donor rate (compound II does not oxidize formate directly).
PerA = peracetate (+ferrocyanide for compound II formation).
Rate and equilibrium constants for fluoride binding are from Fig. 4.
Data for reactions with formate are as described in the text.

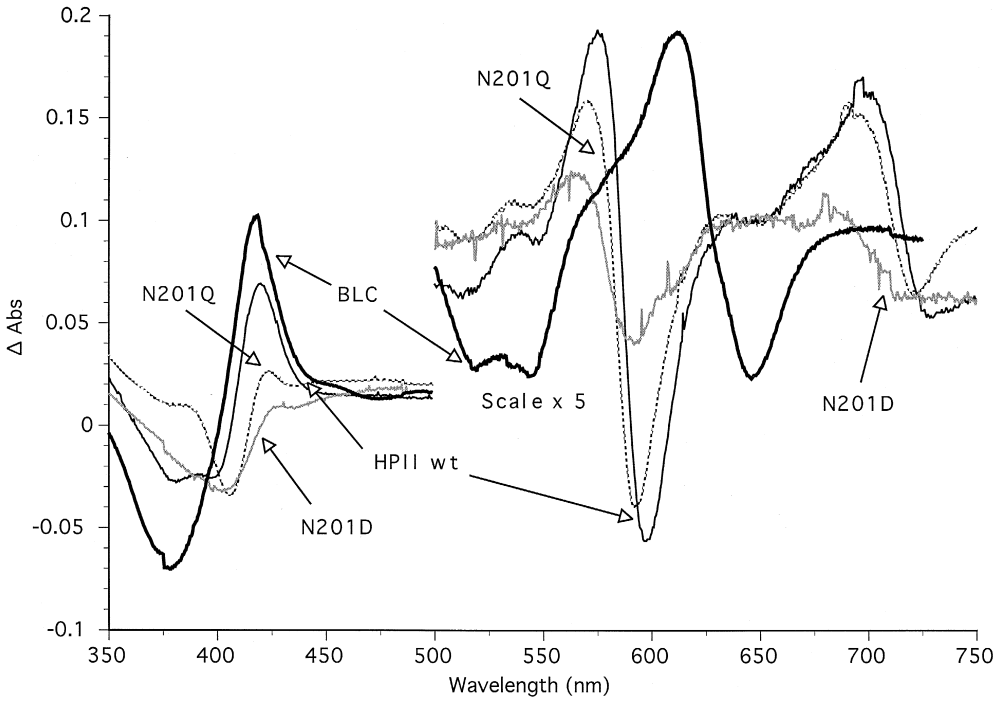

Fig. 5. Difference spectra of catalase–formate complexes. Increasing amounts of formate were added in a step-wise fashion (0.1 to 75 mM Na salt) to the indicated enzyme samples in 100 mM potassium phosphate buffer pH 6.8 at 30°C. HPIIwt, thin black trace: 5 μM HPII wild-type enzyme; N201D, gray trace: 3 μM asn201asp mutant HPII; N201Q, dashed trace: 7 μM asn201gln mutant HPII; BLC, heavy black trace: 5 μM beef liver enzyme. Final spectra computed by extrapolation to infinite [formate] as in Fig. 2, using the parameters for the curves in Fig. 6. Absorbance changes are also adjusted for equal enzyme (heme) concentrations (≈ 7 μM).

ride concentration (Fig. 3). Beef liver enzyme shows a classical sigmoidal fluoride binding curve in both visible and Soret regions (Fig. 3(A)), with K_d (pH 5.0) = 4.2 mM. HPII enzymes showed irregular sigmoidal curves in the Soret region, suggesting molecular heterogeneity, but the wild type HPII and N201Q mutants showed single sigmoid titration patterns in the visible region. Using the visible region data in Fig. 3(B)–(D), the K_d values at pH 5.0 for fluoride complexes of HPII wild-type, N201Q and N201D were found to be 0.16, 0.6 and 6 mM respectively. A small fraction of N201D showed a much higher fluoride affinity further indicating heterogeneity in the heme composition of this mutant. These results are summarized in Table 1.

3.3. Rate of catalase–fluoride complex formation

Fluoride binding to beef liver catalase was monitored by stopped flow kinetics. Typical traces at 595

Table 3
Spectra and affinities of catalase–formate complexes

Catalase	Spectral maxima		Dissociation constants (mM)	
Type	Soret (nm)	Visible (nm)	pH 5.8	pH 6.8
BLC	406	612	0.53	3.9
HPII (WT)	407	550, 630, 701	0.9	7.7
N201D	409	565, 610, 685	ND	134
N201Q	406	582, 630, 700	4.1	57

Spectral peak positions were obtained from the data in Fig. 5. 100 mM potassium phosphate pH 5.8 or 6.8 at 23°C. Other conditions as in Table 2 and Fig. 6.

and 634 nm are shown in Fig. 4(A) and the rates are plotted against fluoride concentration in Fig. 4(B). The k_{on} (second order), k_{off} (first order) and K_d (dissociation) constants obtained at pH 5.8 are listed in Table 2 for comparison with formate (discussed below).

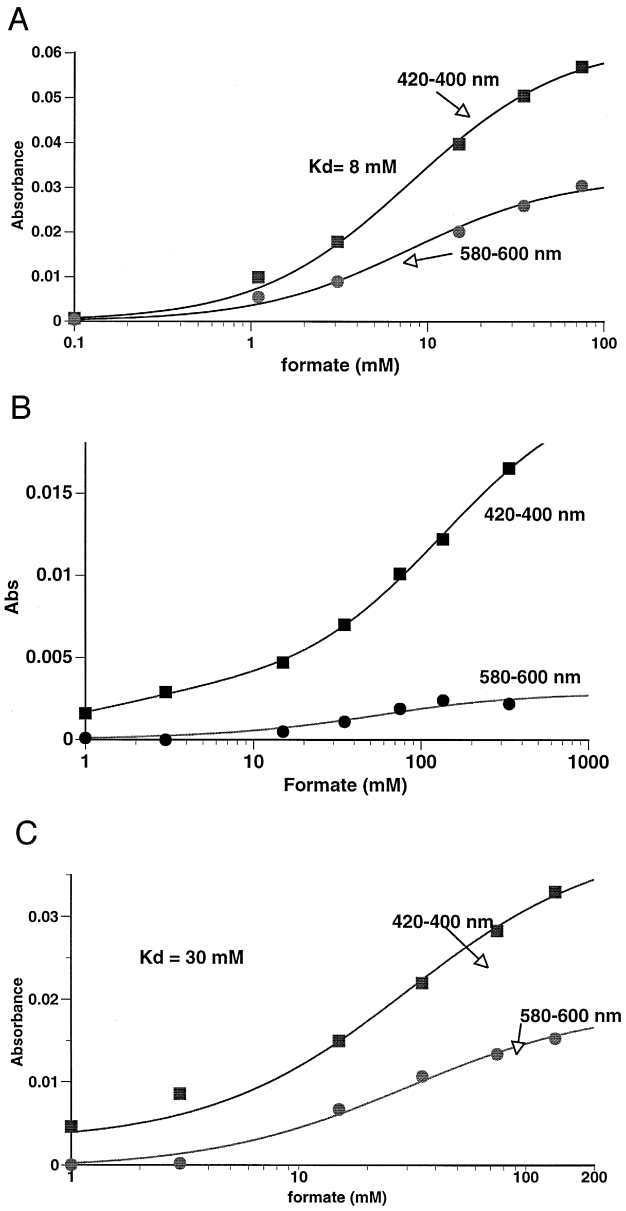

Fig. 6. Formate binding by three HPII catalases. Absorbance change vs. formate concentration for the wavelength pairs 420–400 nm (■) and 580–600 nm (●). 100 mM potassium phosphate buffer pH 6.8 at 30°C. Other conditions are as described in the legend to Fig. 5. (A) HPIIwt, 5 μM HPII wild-type enzyme; (B) N201D, 3 μM asn201asp mutant HPII; (C) N201Q, 7 μM asn201gln mutant HPII.

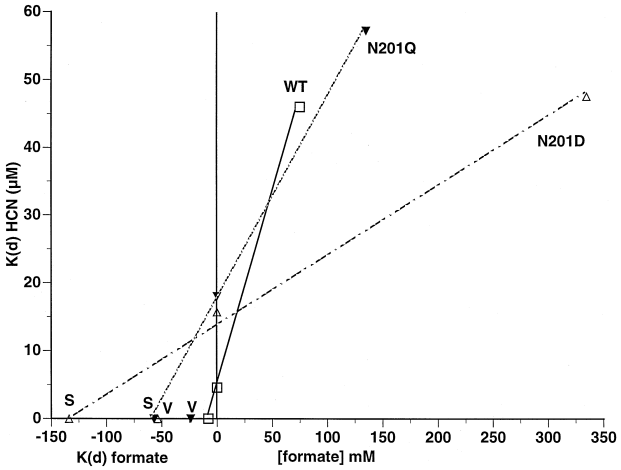

Fig. 7. Competition between cyanide and formate for binding the heme groups of HPII catalase and its mutants. The vertical (Y) axis indicates the dissociation constants for cyanide binding to wild type HPII catalase (WT) and the two mutants (N201Q and N201D), in the absence of formate and in its presence. The horizontal (X) axis indicates the formate concentration. The points on the negative side of this axis indicate the apparent dissociation constants for formate binding in the Soret (S) and visible (V) regions in the absence of cyanide. These plots can be used to determine the formate dissociation constants for the wild type and mutant enzymes as described in the text. Conditions as in Fig. 5 and 6.

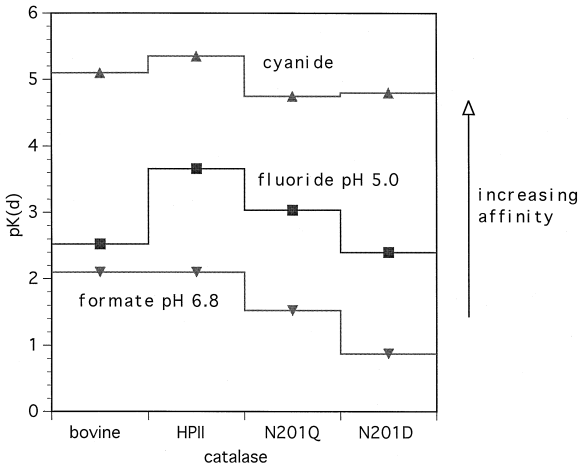

Fig. 8. Summary of observed catalase equilibrium constants. The vertical axis indicates pK_d, the negative logarithm of the calculated dissociation constant. The categories on the horizontal axis are the four catalase types. The cyanide data are as given in Ref. [23].

A previous paper [23] described the slow binding kinetics of cyanide with HPII enzymes. Fluoride binding to HPII catalases, monitored kinetically in the visible and Soret regions, was essentially rapid under ordinary mixing conditions. Sufficient enzyme was not available to test binding kinetics under stopped flow conditions.

3.4. Spectra and kinetics of catalase–formate complex formation

Formate induces a blue shift of the beef liver catalase α-band and a red shift of its Soret band, also indicating high-spin complex formation (Fig. 5). When absorbance in either the Soret (418–380 nm) or

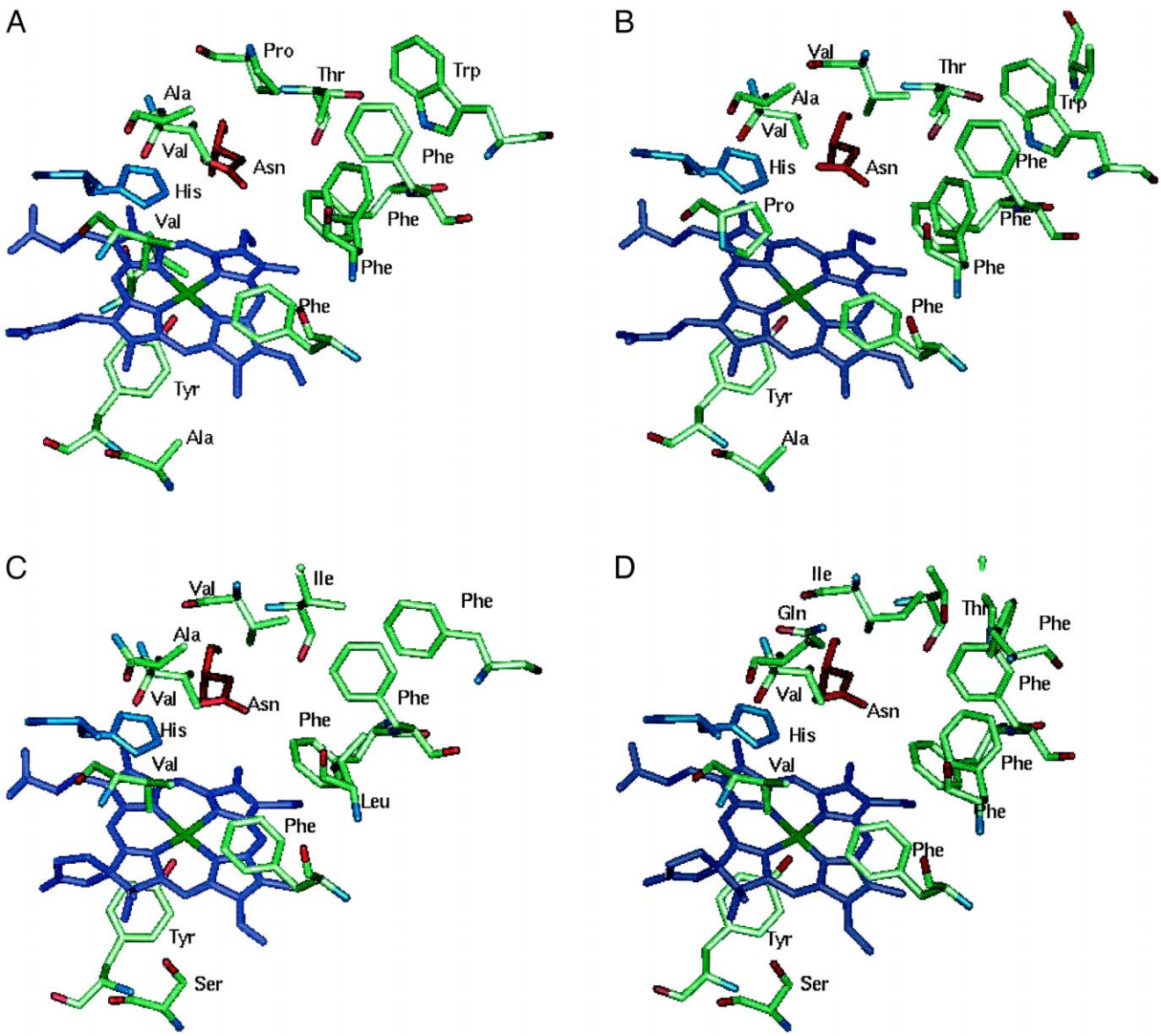

Fig. 9. Active site residues of four catalases The heme environments are shown for: (A) beef liver catalase; (B) *Micrococcus lysodeiktus* catalase; (C) *Penicillium vitale* catalase; (D) *Escherichia coli* HPII catalase. Distal histidines and asparagines are coloured blue and red respectively. Most of the hydrophobic residues which line the channel are conserved. The protoheme enzymes (A) and (B) contain an alanine residue on the distal side of the heme directly below pyrrole ring III. The analogous residue for both heme d enzymes (C) and (D) is serine. This modification in the heme pocket environment may assist conversion of protoheme to heme d [14]. Structural coordinates in Brookhaven Protein Data Bank (pdb) format courtesy of I. Fita and G. Murshadov (see Acknowledgments).

Table 4
Comparison of heme pocket and channel residues

Catalase	Distal residues	Proximal residues	Heme channel residues		
BLC	H74, N147	Y357, A356	G464	V246	A250
MLC	H57, N129	Y399, A338	G448	N228	T232
PVC	H63, N136	Y350, S349	H464[a]	W239[a]	E243[a]
HPII	H128, N201	Y415, S414	F529[a]	W304[a]	Q308[a]

Distal histidine is always ≈4.8 Å from the heme Fe (cf. Fig. 9); distal asparagine is always ≈6 Å from the heme Fe. Tyrosinate always occupies the 5th coordination site. The residue proximal to the 3rd pyrrole is always ≤2.4 Å from the porphyrin ring.
[a] The heme channel entrance (Fig. 10) for heme d enzymes is partially occluded.

visible (612–648 nm) regions is plotted against formate concentration (not shown) pH-dependent catalase–formate dissociation constants (K_d) are obtained as summarized in Tables 2 and 3. These are similar in magnitude to the values previously reported [26]. Formate binding to the ferric enzyme and formate reduction of the primary peroxide compound (compound I, formed either from peroxide itself or by addition of peracetate) can also be followed kinetically using either stopped flow or standard spectrophotometry. As shown in Table 2, the rate constants for these two processes are similar.

Difference spectra of HPII wild-type, N201D and N201Q enzymes complexed with formate are shown in Fig. 5. The α band in each case is blue shifted by 10 nm and the Soret band red shifted by about 1 nm. Absorption peaks and troughs for N201D and its formate complex are broader than for its wild-type and N201Q counterparts, perhaps confirming a heterogeneous heme population. Absorbance changes in Soret (420–400 nm) and visible (580–600 nm) regions were plotted against formate concentration (Fig. 6(A)–(C)). Formate binding to HPII (wild-type), like its reaction with beef liver enzyme, displayed simple saturation kinetics (Fig. 6(A)). Binding to the two HPII mutant enzymes could not be fitted by such a simple equation. Mutant enzyme samples apparently contained at least two populations, with different binding affinities. The data in both the Soret and visible regions (Fig. 6(B) and (C)) could be fitted to Eq. (1)

$$A = \frac{A_{max1} * F}{\{K_{d1} + F\}} + \frac{A_{max2} * F}{\{K_{d2} + F\}}, \quad (1)$$

where A is absorbance, A_{max1} and A_{max2} are maximal changes of absorbance for the two populations, F is the formate concentration and K_{d1} and K_{d2} the apparent dissociation constants for the two populations.

Fitted results (not shown) indicate that the contribution of the smaller population, for both N201D and N201Q, was less than 15% of the total. The dissociation constants for the majority (85% +) population were therefore used for comparative purposes.

A second difficulty was that the dissociation constants obtained from titration curves in the Soret and visible regions were not the same. Another method of determining binding affinities was therefore needed. The method of choice was to probe competition between formate and the low-spin ligand cyanide, the latter being known to occupy the sixth coordination site on the heme iron [23].

3.5. Competition between cyanide and formate for HPII catalase

BLC, HPII wild-type, N201D and N201Q all have similar affinities for cyanide [23]. Preformed HPII catalase–formate complexes were titrated step-wise by additions of cyanide, plotting the changes in absorbance at appropriate wavelength pairs against cyanide concentration. Control titrations with cyanide in the absence of formate were performed as described in Maj et al. [23]. The K_d (cyanide) values

Fig. 10. The access channel configurations. Distal histidines are coloured blue, distal asparagines red. Proximal tyrosines are not shown. Structural coordinates as in Fig. 9. (A). Protoheme catalases (i) beef liver catalase channel stereochemistry; (ii) *M. lysodeikticus* catalase channel stereochemistry. The active site channel for MLC is partially occluded by a short stretch of backbone compared to BLC (shown in pink). (B). Heme d catalases (i) *P. vitale* catalase channel stereochemistry; (ii) *E. coli* HPII catalase channel stereochemistry. The active site channels for PVC and HPII enzymes are partially occluded by a short stretch of backbone (shown in pink). PVC and HPII channels are further occluded by aromatic residues at the entrance of the channel (green and orange residues).

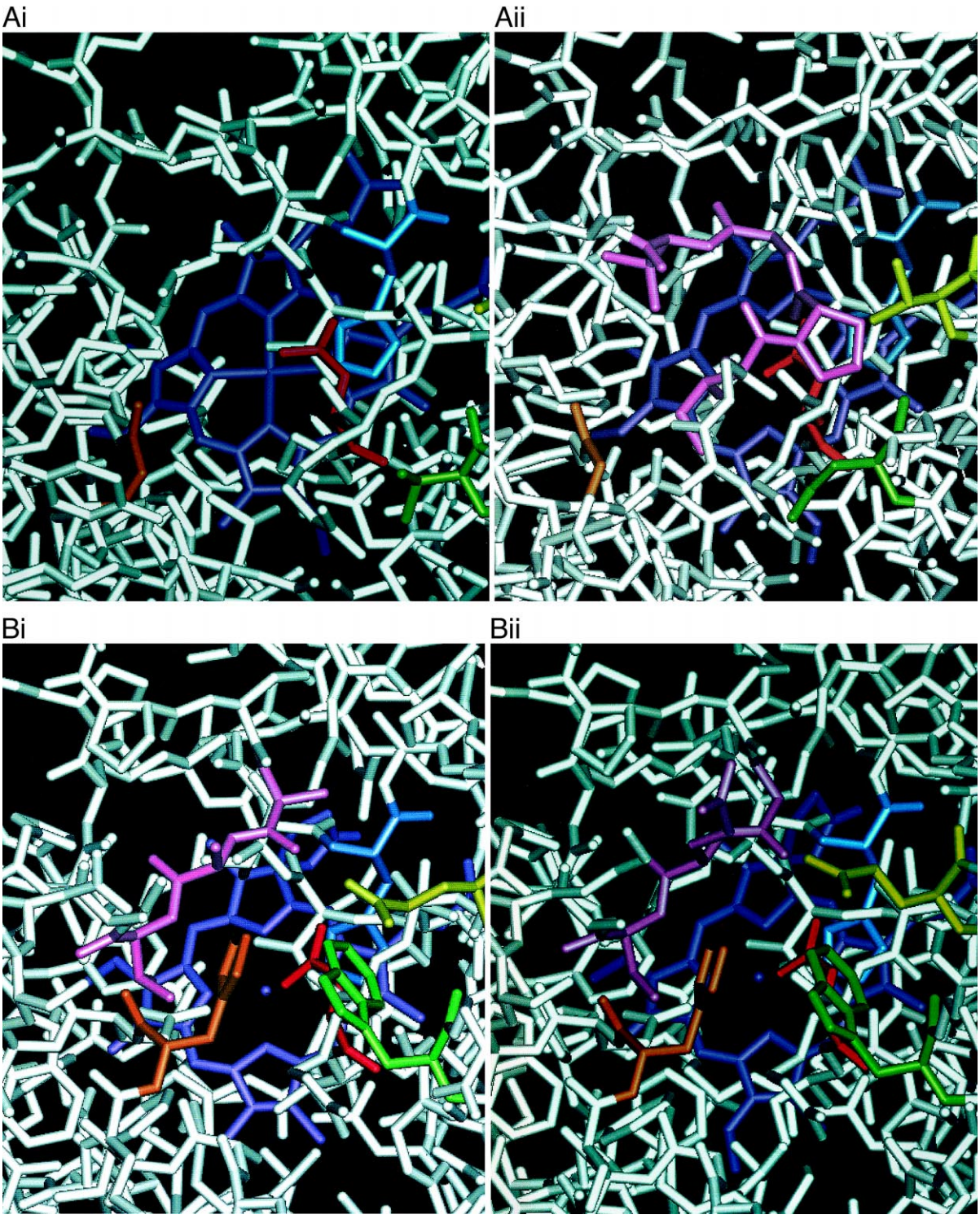
Ai
Aii
Bi
Bii

obtained for HPII wild-type and mutant enzymes are summarized in Figs. 7 and 8 (Section 4). A summary ''Dixon'' plot was then constructed for each HPII enzyme at each pH value tested. The results for the pH 6.8 titrations are shown in Fig. 7, with the dissociation constants for cyanide in the absence of formate plotted on the vertical axis. The K_d (cyanide) is dependent upon the presence of formate. The extrapolated (negative) intercepts on the *x*-axis give the predicted values for the formate dissociation constants in the absence of cyanide. The experimentally determined K_d (formate) values in the Soret and visible regions are also plotted along the (negative) *x*-axis. The competitive K_d (formate) values obtained are summarized in Table 3. These correspond more closely to the lower affinity values determined directly in the Soret region than to those obtained in the visible region.

4. Discussion

4.1. The active site of heme d and protoheme catalases

The crystal structures of the PVC [14] and HPII [9] enzymes show the stereochemistry of the two heme d chiral carbon atoms as identical. The PVC and HPII heme groups are located at similar depths and orientations, but the heme in PVC and HPII is rotated about its *x*-axis by 180° relative to the heme of BLC (i.e. the 5th and 6th coordination positions, or the two heme faces, are interchanged). Residues within contact distance of the heme are somewhat different for heme d and protoheme enzymes. Such residues for HPII include I114, I279, P356 and L407, while analogous residues for BLC are M60, S216, L298 and M349. These differences may determine heme orientation [14].

Both heme d enzymes have a unique serine located just 2 Å below pyrrole ring 3. A hydrogen bond is formed between the hydroxyl group of the heme d and the O-g of this residue (S414 in HPII). Protoheme catalases (beef liver and *Micrococcus*) have an alanine residue in this position. The serine may assist in ring 3 hydroxylation to produce heme d; HPII and *Penicillium* enzymes originally bind protoheme which is converted to heme d during the progress of the catalatic reaction. Ser414 is also H-bonded to the carboxylate oxygen of an aspartate in domain 1 of a neighboring subunit (asp118 in HPII). Such interactions may stabilize heme d with the hydroxyl oxygen pointing toward the proximal side [14,16]. Recent crystal structure and direct analysis also suggests that the proximal tyrosine is covalently bonded to the β-carbon of a proximal histidine residue (His392) in HPII [29]. This is apparently due to a second oxidative step during the conversion of the protoheme-containing ''proenzyme'' to the heme d-containing active enzyme in this system.

The conserved distal histidine and asparagine are at similar orientations within the active site and at similar distances from the heme iron, i.e. 4–5 Å for his and 5.5–6 Å for asn (see Fig. 9). The proximal ligand is always tyrosine. A summary of the key proximal and distal residues for the four enzymes is given in Table 4.

The channels leading from the exterior to the heme pocket, and the active sites of the beef liver, *Micrococcus*, *Penicillium* and HPII enzymes show almost complete homology (cf. Fig. 10(A) and (B)). The heme group is always located some 20–30 Å from the protein surface. The access channel for all four enzymes is lined with mainly hydrophobic residues. Beef liver enzyme is the most solvent accessible. The channel of the catalytically more active (twice that of beef liver) *Micrococcus* enzyme appears to be obstructed by a stretch of protein backbone (Fig. 10(A)) located one third of the distance from the channel entrance. The channels of *Penicillium* and HPII catalases are also obstructed by such a stretch of protein backbone (Fig. 10(B)) and these enzymes contain residues which may block the channel entrance itself, Q308, W304 and F529 in HPII and Q243, W239 and H464 in *Penicillium.* A summary of this structural information is also provided in Table 4.

4.2. Ligand binding by catalases with different heme pockets

Fig. 8 summarises the differences in equilibrium binding of three ligands by the four catalases – beef liver enzyme and three forms of *E. coli* HPII. The low-spin ligand cyanide inhibits both prokaryotic and eukaryotic catalases. As shown in Fig. 8, and reported previously [23], protoheme, heme d and mu-

tant enzymes have similar cyanide affinities. However, heme d enzymes bind cyanide much more slowly than does the beef liver enzyme [23]. The affinity is probably governed by heme iron chemistry and not by the heme pocket. Resonance Raman spectra of cyanide-ligated beef liver and *A. niger* catalases have suggested that cyanide can bind with two geometries, one linear and the other bent. Such heterogeneity may indicate H-bonding to two alternative distal residues [30]. The linear conformer with stretching and bending frequencies at 434 and 413 cm^{-1} probably involves hydrogen bonding to the distal histidine. The bent conformer with stretching and bending frequencies at 445 and 456 cm^{-1} is obtained when pH > 8 and the distal histidine may be deprotonated. This could involve the distal asparagine. HCN ligation in two conformational states was also reported for plant peroxidase [31,32].

Reactions of fluoride and formate with catalase are both pH dependent. As the *p*K of hydrofluoric acid is 3.45 and that of formate 3.75 [33], the present work was carried out under conditions in which the ligands were primarily in their anion forms. It has confirmed the classical finding that the affinities of formate and fluoride for catalases increase as pH is lowered, and extended this observation to include the *E. coli* enzyme HPII. In contrast, the K_d values for cyanide interaction with catalase, whether from beef liver or *E. coli*, vary only slightly between pH 5.8 and pH 6.8. Binding of all these ligands thus involves uptake of both an anion and a proton into the heme pocket.

HPII (wild type) has a ten-fold higher affinity for fluoride than does beef liver enzyme. The heme d pocket may provide a polar environment favourable to fluoride binding. Mutation of distal asparagine to glutamine decreases fluoride affinity, probably a consequence of steric effects. The probable negative environment provided by substitution of asparagine with aspartic acid further decreases fluoride affinity, an effect which may be electrostatic in character.

Formic acid, unlike hydrofluoric acid, resembles hydrogen peroxide structurally. The affinity of the HPII wild-type enzyme for formate is lower than that of the mammalian enzyme. Occlusion of the heme channel by bulky side chains (see below) may contribute to this lower affinity. The asparagine to glutamine and asparagine to aspartate mutants also showed decreases in formate affinity (Fig. 8). These differences parallel the declines in catalytic activity of the mutants [16].

4.3. Ligand competition

The cyanide-induced changes in the spectra of the catalase–formate complex support the idea that formate and cyanide compete for a common heme binding site. Mutation of the distal asparagine does not affect the cyanide affinity but it does change the affinity for high-spin ligands. The formate reaction was more sensitive than that of fluoride, suggesting that stabilization of formate in the heme pocket is energetically more dependent on the distal asparagine residue.

We conclude that the catalases show similar affinities for the low-spin ligand cyanide, though the bacterial enzymes bind cyanide approximately 1000 times more slowly [23]. Amino acids distal to the heme control high-spin ligand complex formation, with both fluoride and formate complexes being more sensitive to changes of the electrostatic environment than to steric modifications of the binding site.

Acknowledgements

We thank Mr. Jacek Switala (University of Manitoba, Winnipeg, Man., Canada) for preparing the samples of *E. coli* HPII catalase and mutants, Dr. I. Fita (University of Barcelona, Spain) for providing HPII X-ray crystal structure coordinates prior to deposition in the Protein Data Bank and Dr. Garib Murshudov of York University (UK) for supplying the coordinates of the *Micrococcus* and *Penicillium* enzymes prior to deposition. This work was supported by research and equipment grants to P.N. and P.L. from the Canadian Natural Sciences and Engineering Research Council and by a Brock University Scholarship to M.M.

References

[1] O. Loew, U.S. Dept. Agric. Reports No. 68, 1901, p. 47.
[2] K. Zeile, H. Hellstrom, Z. Phys. Chem. 192 (1930) 171.
[3] J.B. Sumner, A.L. Dounce, J. Biol. Chem. 121 (1937) 417–424.

[4] R.K. Bonnichsen, B. Chance, H. Theorell, Acta Chem. Scand. 1 (1947) 685–709.
[5] A. Deisseroth, A.L. Dounce, Physiol. Rev. 50 (1970) 319–375.
[6] G.R. Schonbaum, B. Chance, Catalase, in: P.D. Boyer (Ed.), The Enzymes, vol. XIII pt. C, 3rd ed., Academic Press, London, 1976, pp. 363–408.
[7] I. von Ossowski, G. Hausner, P.C. Loewen, J. Mol. Evol. 37 (1993) 71–76.
[8] M.R.N. Murthy, T.J. Reid, A. Sicignano, N. Tanaka, M.G. Rossmann, J. Mol. Biol. 152 (1981) 465–499.
[9] J. Bravo, N. Verdaquer, J. Tormo, C. Betzel, J. Switala, P.C. Loewen, I. Fita, Structure 3 (1995) 491–502.
[10] G.N. Murshudov, W.R. Melik-Adamyan, A.I. Grebenko, V.V. Barynin, A.A. Vagin, B.K. Vainshtein, Z. Dauter, K.S. Wilson, FEBS Lett. 312 (1992) 127–131.
[11] R.K. Vainshtein, W.R. Melick-Adamyan, V.V. Baryin, A.A. Vagin, M.G. Rossmann, J. Mol. Biol. 188 (1986) 49–61.
[12] W.R. Melik-Adamyan, V.V. Baryin, A.A. Vagin, V.V. Borisov, B.K. Vainshtein, I. Fita, M.R.N. Murthy, M.G. Rossman, J. Mol. Biol. 188 (1986) 63–72.
[13] P. Gouet, H.M. Jouve, O. Dideburg, J. Mol. Biol. 249 (1995) 933–954.
[14] G.N. Murshudov, A.I. Grebenko, V. Barynin, Z. Dauter, K.S. Wilson, B.K. Vainshtein, W. Melik-Adamyan, J. Bravo, J.M. Ferran, J.C. Ferrer, J. Switala, P.C. Loewen, I. Fita, J. Biol. Chem. 271 (1996) 8863–8868.
[15] R. Timkovich, L.L. Bondoc, Adv. Biophys. Chem. 1 (1990) 203–247.
[16] P.C. Loewen, J. Switala, I. von Ossowski, A. Hillar, A. Christie, B. Tattrie, P. Nicholls, Biochemistry 32 (1993) 10159–10164.
[17] I. Fita, M.G. Rossman, J. Mol. Biol. 185 (1985) 21–37.
[18] L.A. Andersson, A.K. Johnson, M.D. Simms, T.R. Willingham, FEMS Lett. 370 (1995) 97–100.
[19] P.C. Loewen, J. Switala, Biochem. Cell Biol. 64 (1986) 638–646.
[20] J.T. Chiu, P.C. Loewen, J. Switala, R.B. Gennis, R. Timkovich, J. Am. Chem. Soc. 111 (1989) 7046–7050.
[21] C. Obinger, M. Maj, A. Hillar, P.C. Loewen, P. Nicholls, Arch. Biochem. Biophys. 342 (1997) 58–67.
[22] P. Nicholls, Biochem. J. 81 (1961) 374–635.
[23] M. Maj, P. Nicholls, C. Obinger, A. Hillar, P. Loewen, Biochim. Biophys. Acta 1298 (1996) 241–249.
[24] M. Maj, P. Nicholls, (1996a) 39th Annual Meeting of the Canadian Federation of Biological Societies, London, Ont. Abst. #111.
[25] M. Maj, P. Nicholls, IV International Symposium on Plant Peroxidases: Biochemistry and Physiology, Abst. #PA-34, Vienna, Austria, 1996.
[26] P. Nicholls, G.R. Schonbaum, Catalases, in: Lardy et al. (Eds.), The Enzymes, 2nd ed., vol. 8, Academic Press, New York, 1963, pp. 147–222.
[27] J.H. Dawson, A.M. Bracete, A.M. Huff, S. Kadkhodayan, C.M. Zeitler, M. Sono, C.K. Chang, P.C. Loewen, FEMS Lett. 295 (1991) 123–126.
[28] R.F. Beers, I.W. Sizer, J. Biol. Chem. 195 (1952) 133–140.
[29] J. Bravo, I. Fita, J.C. Ferrer, W. Ens, A. Hillar, J. Switala, P.C. Loewen, Protein Sci. 6 (1997) 1016–1023.
[30] J. Al-Mustafa, M. Sykora, J.R. Kincaid, J. Biol. Chem. 270 (1995) 10449–10460.
[31] J. Al-Mustafa, J.R. Kincaid, Biochemistry 33 (1994) 2191–2197.
[32] S. Han, J.F. Madden, I.M. Siegen, T.G. Spiro, Biochemistry 28 (1989) 5477–5485.
[33] D.R. Linde, CRC Handbook of Chemistry and Physics, 71st ed., CRC Press, Boca Raton, 1990, pp. 36–37.